ANNUAL REVIEWS

Annual Review of Physical Chemistry

Prebiotic Astrochemistry from Astronomical Observations and Laboratory Spectroscopy

Lucy M. Ziurys

Department of Chemistry and Biochemistry, Department of Astronomy, and Steward Observatory, University of Arizona, Tucson, Arizona, USA; email: lziurys@arizona.edu

ANNUAL REVIEWS CONNECT
www.annualreviews.org
• Download figures
• Navigate cited references
• Keyword search
• Explore related articles
• Share via email or social media

st (guest) IP: 174.18.91.56 On: Fri, 09 May 2025 21:45:19

Annu. Rev. Phys. Chem. 2024. 75:307–27

First published as a Review in Advance on February 21, 2024

The *Annual Review of Physical Chemistry* is online at physchem.annualreviews.org

https://doi.org/10.1146/annurev-physchem-090722-010849

Copyright © 2024 by the author(s). This work is licensed under a Creative Commons Attribution 4.0 International License, which permits unrestricted use, distribution, and reproduction in any medium, provided the original author and source are credited. See credit lines of images or other third-party material in this article for license information.

OPEN ACCESS CC BY

Keywords

astrochemistry, spectroscopy, millimeter wave, microwave, radio astronomy, prebiotic chemistry, Solar System

Abstract

The discovery of more than 200 gas-phase chemical compounds in interstellar space has led to the speculation that this nonterrestrial synthesis may play a role in the origin of life. These identifications were possible because of laboratory spectroscopy, which provides the molecular fingerprints for astronomical observations. Interstellar chemistry produces a wide range of small, organic molecules in dense clouds, such as NH_2COCH_3, CH_3OCH_3, CH_3COOCH_3, and $CH_2(OH)CHO$. Carbon (C) is also carried in the fullerenes C_{60} and C_{70}, which can preserve C-C bonds from circumstellar environments for future synthesis. Elusive phosphorus has now been found in molecular clouds, the sites of star formation, in the molecules PO and PN. Such clouds can collapse into solar systems, although the chemical/physical processing of the emerging planetary disk is uncertain. The presence of molecule-rich interstellar starting material, as well as the link to planetary bodies such as meteorites and comets, suggests that astrochemical processes set a prebiotic foundation.

1. THE EMERGENCE OF ASTROCHEMISTRY

The chemical richness of interstellar space has been realized only in the past few decades. Because astronomy relies on remote sensing across enormous distances, gas-phase spectroscopy has always been the major tool for investigating the composition of the interstellar medium (ISM), the vast regions between stars. Prior to the 1970s, it was thought in the astronomical community that the ISM could harbor only atomic material, with perhaps a handful of diatomic molecules. During the 1940s, several such molecules, including CH, CH^+, and CN, were identified in the ISM via their electronic bands, observed at optical wavelengths in absorption against background stars (e.g., 1). These discoveries were considered more spectroscopic curiosities than clues to further molecular content. It was not until approximately 20 years later, with the development of radio astronomy coupled with progress in laboratory microwave spectroscopy (2), that the overall landscape changed. With the availability of rotational rest frequencies from laboratory measurements, as well as sensitive heterodyne electronics (e.g., 3), molecular detections began to occur at radio wavelengths, starting with the OH radical (4) and quickly followed by H_2O, NH_3, and H_2CO (3–5). These pioneering identifications were made on the basis of lambda doubling, inversion doubling, and K doubling, which limited the accessible molecules. The discovery of carbon monoxide (CO) in the Galaxy further revolutionized molecular astronomy (6) by opening the sky to millimeter wavelengths. CO was identified by its $J = 1 \rightarrow 0$ rotational line at 115 GHz. It was soon recognized that millimeter wavelengths offered the best access to molecular transitions. Discoveries came rapidly thereafter, with the detections of HCN, HNC, HCO^+ (known as Xogen), H_2S, CS SiO, CH_3CH, and HNCO (e.g., 7–9).

Fifty years later, more than 200 interstellar molecules have been identified in interstellar space on the basis of their gas-phase spectra. A wide range of chemical species have been observed, from simple diatomics such as NO, SO, SiC, NH, and OH to more complex compounds such as CH_3NH_2 (10), CH_3CONH_2 (11), and $CHOCH_2OH$ (12). The largest gas-phase molecules observed to date are C_{60}, C_{70} (13), and possibly C_{60}^+ (14). Most species have been detected by their rotational transitions in the millimeter range (65–500 GHz), using high-precision radio telescopes (15). Sample spectra are shown in **Figure 1**. Rotational lines are favored because interstellar gas is typically cold (~10–100 K) and constitutes a near vacuum (10^3–10^6 particles/cm^3 or 10^{-17}–10^{-14} atm). However, this method requires that a molecule have a permanent electron dipole moment. The infrared (IR) region has therefore played an important role in the identification of very symmetric species, from CH_4, SiH_4, and HCCH to C_{60}, by exploiting ro-vibrational transitions (16, 17). Detection in the IR is usually more selective because it requires a radiation source for excitation, while rotational levels are simply populated by collisions with the most abundant molecule, H_2 (18). A few molecules, such as NH and C_2, have been identified by their electronic bands in the near-IR and optical regions of the electronic spectrum (19, 20). Usually, these studies are done in absorption against a background star for excitation.

Table 1 shows a representative list of known interstellar molecules. A complete current list is given in **Supplemental Table 1**. Approximately half of all known interstellar molecules are transient species that would likely function as short-lived reaction intermediates in the terrestrial laboratory. These unusual molecules include free radicals such as CCH, HCO, SiC, and CCP and both positive and negative molecular ions (e.g., HCO^+, $HCNH^+$, C_3N^-). The presence of these nonterrestrial compounds arises from the very rarefied and cold gas that hosts them. A variety of elements are contained in the molecules, starting with NCHOPS (nitrogen, carbon, hydrogen, oxygen, phosphorus, sulfur)—the elements thought necessary for life (21). In fact, most interstellar molecules contain C and common organic functional groups, with acids, alcohols, aldehydes, ketones, esters, and amines (22). N, O, and S are also reasonably well represented, and a few molecules

Supplemental Material >

Downloaded from www.annualreviews.org. Guest (guest) IP: 174.18.91.56 On: Fri, 09 May 2025 21:45:19

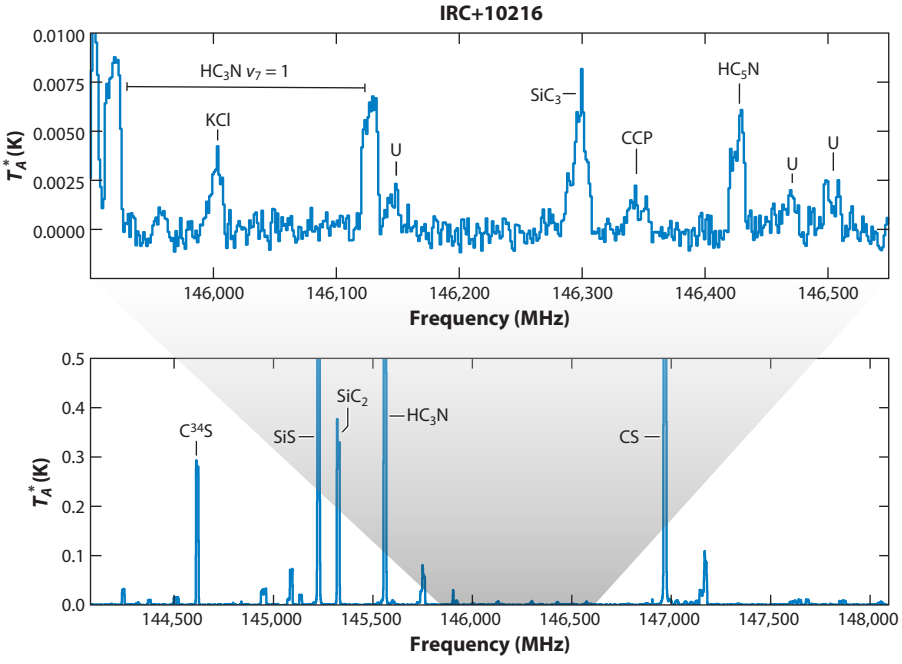

Figure 1

Representative millimeter-wave spectra of the C-rich envelope of IRC+10216 at 2 mm in wavelength. (*Lower*) A spectrum at 146 GHz with a 4-GHz total bandwidth, showing the strong spectral lines in this region, including those of $C^{34}S$, CS, SiS, SiC_2, and HC_3N. The spectral intensity scale [in T_A^* (K)] has been truncated to show weaker features. These data were taken with the 12-m telescope of the Arizona Radio Observatory with 56 h of integration time. (*Upper*) A section of the lower spectrum with a bandwidth of 0.5 GHz. Weaker lines are apparent in the spectrum. U denotes unidentified lines.

have fluorine (F) and chlorine (Cl) [HCl, CF, CF^+, H_2Cl^+ (23)]. P has been more elusive and has been found in only seven interstellar molecules to date (see **Table 2**). Of the more refractory elements, silicon (Si) is the most prevalent in molecular form as diatomics (SiO, SiC, SiN, SiS, SiP) and in organosilicon species (SiC_3, SiC_4, SiNC). The metals, in the chemist's sense, are represented in molecules by magnesium (Mg), aluminum (Al), sodium (Na), potassium (K), titanium

Table 1 Representative interstellar molecules

Two elements		Three elements		Four elements	Five elements	Six elements	Seven elements	Eight or more elements
H_2	PN	HCO^+	SiC_2	H_2CO	HC_3N	CH_3OH	CH_3CCH	$HCOOCH_3$
CO	PO	HCN	OCS	HCCH	CH_2CN	CH_3CN	HC_5N	CH_3CH_2CN
CN	AlF	N_2O	CCN	H_3O^+	C_4H	C_5H	C_6H^-	CH_3CH_2OH
NO	NaCl	CCH	HNC	$HCNH^+$	HCOOH	NH_2CHO	CH_2CHCN	HC_7N
OH^+	AlO	HNO	AlNC	C_3H	H_2COH^+	C_5N^-	CH_3CHO	$(CH_2OH)_2$
SiO	SiC	H_2O	MgCN	NH_3	CH_4	C_2H_4	CH_3NH_2	HC_9N
NH	VO	H_2S	FeCN	HSCN	SiH_4	CH_3SH	CH_3NCO	C_8H
HCl	ArH^+	N_2H^+	AlOH	PH_3	c-C_3H_2	c-H_2C_3O	C_6H	C_{60}
NS	TiO	CCP	HNO	C_3O	C_4H^-	MgC_4H	c-C_2H_4O	C_{70}

Downloaded from www.annualreviews.org. Guest (guest) IP: 174.18.91.56 On: Fri, 09 May 2025 21:45:19

Table 2 A summary of phosphorus chemistry

Species	Source type	Source	$f(X/H_2)$[a]	$f(X/H_2)$ range
PN	C-rich AGB envelope	IRC+10216	9×10^{-10}	$0.09–2 \times 10^{-8}$
	O-rich AGB envelope	TX Cam IK Tau R Cas	10^{-8} 10^{-8} 2×10^{-8}	
	Hypergiant envelope	VY CMa NML Cyg	8×10^{-8} 3×10^{-9}	
	Protoplanetary nebula	CRL2688	$3–5 \times 10^{-9}$	
	Clouds: high-mass star Formation	Orion-KL W51 W3 (OH)	6×10^{-11} 10^{-10} 4×10^{-11}	$0.4–9 \times 10^{-10}$
	Clouds: low-mass star Formation	B-1 L1157	10^{-10} 9×10^{-10}	
PO	O-rich AGB envelope	TX Cam IK Tau R Cas	6×10^{-8} 5×10^{-8} 10^{-7}	$0.5–1 \times 10^{-7}$
	Hypergiant envelope	VY CMa NML Cyg	10^{-7} 7×10^{-8}	$0.7–1 \times 10^{-7}$
	Clouds: high-mass star Formation	Orion-KL W51 W3 (OH)	2×10^{-10} 2×10^{-10} 10^{-10}	$1–2 \times 10^{-10}$
	Clouds: low-mass star Formation	B-1 L1157	10^{-10} 2×10^{-10}	
PH_3	C-rich AGB envelope	IRC+10216	10^{-8}	$0.1–4 \times 10^{-7}$
	Protoplanetary nebula	CRL 2688	$0.3–4 \times 10^{-7}$	
HCP	C-rich AGB envelope	IRC+10216	3×10^{-8}	$0.3–2 \times 10^{-7}$
	Protoplanetary nebula	CRL 2688	2×10^{-7}	
CP	C-rich AGB envelope	IRC+10216	7×10^{-9}	
CCP	C-rich AGB envelope	IRC+10216	1×10^{-9}	
SiP	C-rich AGB envelope	IRC+10216	2×10^{-9}	

[a]Abundance relative to H_2.
[b]Data from References 136 and 139–144.
Abbreviations: AGB, asymptotic giant branch; IK Tau, IK Tauri; NML Cyg, NML Cygnus; R Cas, R Cassiopeiae; TX Cam, TX Camelopardalis; VY CMa, VY Canis Majoris.

(Ti), iron (Fe), and (most recently) vanadium (V). Mg, the metal most common in interstellar molecules, is found in, e.g., MgCN, MgCN, MgC_2, and MgC_4H (24), while V and Fe have thus far been observed only in VO (25), FeCN (26), and recently FeC, respectively. Also of interest is the presence of ArH^+ (27).

2. THE INTERSTELLAR MOLECULAR LIFE CYCLE

The wide variety of molecules observed are not found in the same sources in the ISM but rather are found in sample different regions with varying physical conditions. These sources are linked together through the transfer of material in the ISM in a continuing cycle, following the birth and death of stars. This cycle is illustrated in **Figure 2**.

Downloaded from www.annualreviews.org. Guest (guest) IP: 174.18.91.56 On: Fri, 09 May 2025 21:45:19

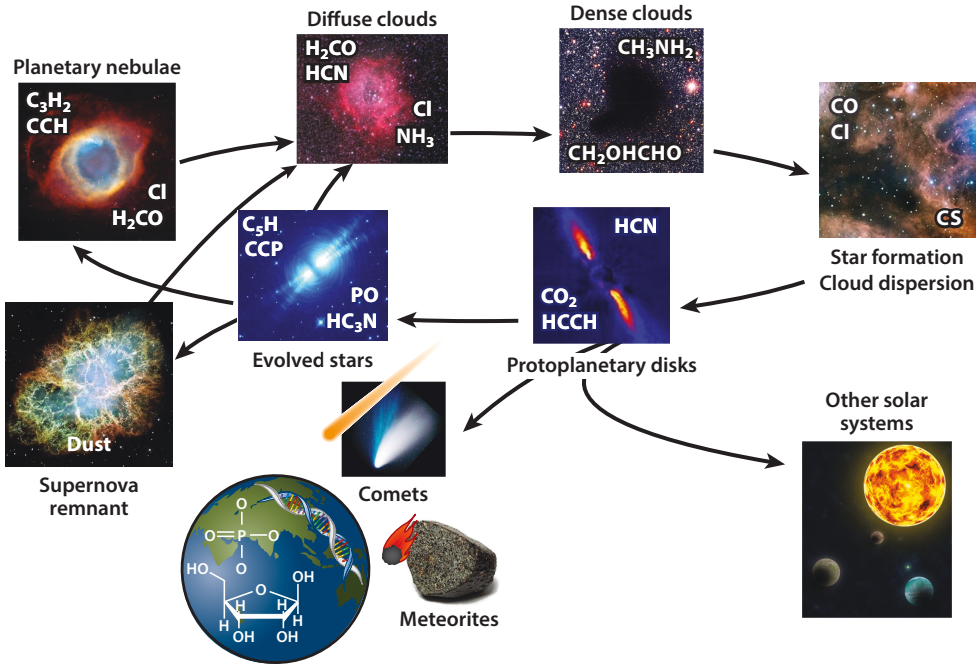

Figure 2

The life cycle of molecules in the Galaxy, illustrating the connection between material lost from evolved stars, and between material in diffuse and dense clouds, and solar systems.

Most elements are supplied to the ISM from stars and either are dispersed in a supernova explosion or enter the ISM through less violent mass loss from asymptotic giant branch (AGB) stars. Supernovae (SNe) are relatively rare in our Galaxy, as they originate in very massive stars (28). While SNe provide approximately 10% of the total mass to the ISM (29), they are the only sources of many heavier elements, even P (30). However, now it is thought that not all massive stars become SNe but that many such stars quietly collapse into black holes (31).

Approximately 85% of the matter in the ISM comes from AGB stars, which—with a typical mass of ∼1–8 $M_\odot$, where $M_\odot$ is the mass of the sun—have lower mass than do SNe progenitors. These AGB objects end their life cycle not explosively, but through a series of stages termed the Giant Branches (see Reference 32). To summarize, these lower-mass stars first deplete H in their core, which is converted to helium (He). They continue to burn H in a shell around the He core until gravitational collapse ignites the He. He burns to C through the triple alpha process. To balance the excess energy released in He burning, the outer layers of the star expand, and a Red Giant star is created. During this phase, the stellar envelope becomes highly convective and mixes material from the H-burning shell to the surface—an important source of ^{13}C. The He core is then transformed to C, and nucleosynthesis continues around it in a He-burning shell that is surrounded by a H-burning shell. This stage is the AGB. Again, the envelope remains highly convective, and a substantial amount of ^{12}C, formed from He, can be dredged up, i.e., mixed to the surface, creating a so-called C star (32)—the only situation known in the ISM in which C > O (C/O ∼ 1.5). This process is termed the third dredge-up. On the AGB, due to energy considerations, mass loss from the surface of the star becomes substantially higher, with expansion velocities near V_{exp} ∼ 10–20 km/s (33), which creates a substantial circumstellar envelope. The envelope cools, and molecules form.

Downloaded from www.annualreviews.org. Guest (guest) IP: 174.18.91.56 On: Fri, 09 May 2025 21:45:19

Circumstellar envelopes of AGB stars are complex chemical factories (34–36). The most-studied example is the envelope of the carbon star IRC+10216 (see **Figure 1**), which is rich in C-containing compounds (36). It is now recognized that very massive stars ($\geq$20 $M_\odot$), so-called hypergiants, such as VY Canis Majoris (VY CMa) and NML Cygnus (NML Cyg), also have molecularly rich envelopes (35, 37–38). These envelopes are created by sporadic, asymmetric mass loss events that are generated by photospheric activity originating in large convection cells (39). However, because hypergiant stars do not undergo third dredge-up, they remain O rich (C/O $\sim$ 0.5). Their envelope chemistry reflects this ratio, with many oxide molecules (40).

In addition to having gas-phase composition, circumstellar shells are active producers of dust grains. These particles, typically 0.1–10 μm in size, are mineral in composition and contain many refractory elements, such as iron, magnesium, and titanium (41, 42). The type of grains created depends on the C/O ratio. Common minerals thought to form in the O-rich envelopes under conditions of local thermodynamic equilibrium (LTE) are $MgAl_2O_4$ (spinel), Al_2O_3 (corundum), $MgSiO_3$ (enstatite), and $CaTiO_3$ (perovskite), while in the C-rich case, SiC, graphite, and metal carbides, sulfides, and nitrides are found (TiC, AlN, FeS). Some LTE predictions have been verified by IR observations of lattice vibrations [Si-O and Si-C stretches, 9 and 11 μm (43)] or by chemical analysis of presolar grains—dust particles extracted from meteorites (44). However, it is not clear that all grains form under LTE conditions; shock waves generated by stellar pulsations and mass loss can cause significant deviations (45). The presence of many gas-phase refractory-type circumstellar molecules is also evidence for non-LTE environments.

The molecular material and dust from circumstellar shells are eventually dispersed into the ISM. For AGB stars, this process occurs through the planetary nebulae (PNe) stage (**Figure 2**). Here these dying stars continue to eject material until the inner core is exposed and they collapse into white dwarfs (46). The mass of these objects is $\sim$0.5 $M_\odot$. Therefore, significant material enters the ISM through PNe. As the stars evolve into white dwarfs, they become strong emitters of UV radiation, which has been thought to destroy most of the molecules in the dispersing AGB shell (47). However, extensive observations have shown that this widespread destruction does not occur; rather, the ejected material enters the diffuse ISM as molecules mixed with dust (48–50). Classic examples of molecule-rich PNe are the Helix Nebula, M2-48, and K4-47, which are approximately 12,000, 4,800, and 1,000 years old, respectively. Presumably the ejecta of a hypergiant star follows a similar course when it collapses to a black hole. A supernova blast wave, in contrast, will obliterate surrounding material, reducing it to an atomic and ionized state (51).

This rich mix of molecules and dust from PNe forms the basis of diffuse clouds. These rarefied objects typically have temperatures near 100 K and densities of $n \sim$ 1–10 particles/cm^3—conditions that make them unsuitable for the production of polyatomic molecules (52). Yet these clouds contain species as complex as CH_3CN and H_2CO (52, 53). Such polyatomic molecules cannot be produced in situ but are likely remnant circumstellar compounds that are transported through the PNe and nonexplosive hypergiant phase.

Diffuse clouds gravitationally collapse into dense clouds (54), generating gas with $n \sim 10^4$–10^7 particles/cm^{-3}. The chemical jump start from diffuse clouds results in these objects having a rich and diverse synthesis, characterized by organic compounds such as alcohols (CH_3OH, EtOH), acids (HCOOH, CH_3COOH), aldehydes and ketones (H_2CO, CH_3CHO), ethers (CH_3OCH_3), and esters (CH_3OCHO, CH_3OCOCH_3). The strong appearance of organic functional groups distinguishes these clouds from C-rich envelopes, in which most of the O is contained in CO and C chain species are common (55, 56). The chemistry is further enhanced in clouds where stars are forming from gravitational collapse, heating up surrounding material. Such regions, termed hot cores, appear to be particularly rich in more complex chemical compounds that likely result from

Downloaded from www.annualreviews.org. Guest (guest) IP: 174.18.91.56 On: Fri, 09 May 2025 21:45:19

these regions' higher temperatures (57–59). Chemical complexity appears to reach its maximum in hot cores.

As stars form, rotation can occur, and conservation of angular momentum leads to the formation of a protostellar disk (60). This disk is composed of material from the nascent molecular cloud. From such a disk, planets can be generated, forming a solar system (60). The molecular cloud gas and dust undergo significant chemical and physical processing in the disk (61–63). The processes are complicated, involving gas-phase and gas-surface reactions in the molecular matter, as well as condensation or freeze-out on grains. The grains coagulate into larger grains and eventually form pebbles. There are also vertical and horizontal drifts in the disk material. Matter brought closer to the star will be heated by stellar UV and X-ray radiation, causing evaporation of condensates and further processing at elevated temperatures; the material flowing upward from the disk will be subjected to ambient starlight and cosmic rays.

Planets form in the disk on the basis of the local composition and physical conditions, although migration in a given solar system can occur (64). Some planets will be rocky like the Earth, and others will be gaseous giants comparable to Jupiter. The Earth formed hot, however, with an atmosphere of mainly CO (65). Because there is little evidence of C in the Earth's crust, it is thought that much of this element was ejected in gaseous molecules from the hot atmosphere (66). Large amounts of C and H_2O were likely brought back to Earth during the period of late heavy bombardment (LHB), approximately 4 billion years ago. LHB peppered the planet with material from comets, meteorites, and asteroid fragments (67). The bombarding material was largely space debris from the molecular cloud in which the Solar System formed. Although the details are subject to debate, the LHB may have brought critical material for living systems to early Earth; it may not be coincidental that life evolved shortly after the LHB.

3. THE PREBIOTIC NATURE OF INTERSTELLAR CHEMISTRY

The connection between the molecular cloud, the emerging Solar System, and the so-called soup that may have led to biological molecules on Earth suggests that interstellar chemistry played a prebiotic role. Interstellar space is a vast synthetic factory with unknown limits to molecular complexity, with large quantities of gas-phase molecules and dust. Furthermore, most interstellar and circumstellar molecules contain C. In fact, they contain all the NCHOPS elements, as discussed (21), although P is still fairly rare. Furthermore, the identification of C_{60}, C_{70}, and possibly C_{60}^+ (13, 14) indicates that large assemblies of C atoms can be formed. The fullerenes are observed primarily in C-rich circumstellar material (68), where C > O. Although not particularly reactive on Earth, these species may be important carriers of C-C bonds that are later processed into organic species, preventing the C from being scavenged by O.

The chemistry occurring in interstellar space is so vast that it would seem unlikely that interstellar molecular material is completely degraded into the atomic state and that chemistry starts over on a planetary surface. The cycling of interstellar material suggests that there is continuity and even a continuum in molecule formation. There is evidence for this continuity from meteorite analysis. Isotope ratios (D/H, $^{12}C/^{13}C$, $^{14}N/^{15}N$) found in organic molecules extracted from pristine meteorites suggest an interstellar origin for these compounds. For example, a deuterium (D) enrichment as large as $\delta D = +7{,}200‰$ (or $D/H \sim 0.0012$) has been found for 2-amino isobutyric acid (69), and $D/H \sim 0.003$ in insoluble organic matter (70). The standard terrestrial value is $D/H = 0.00015$. Very high D/H ratios are often observed in cold molecular clouds, with values ranging from 0.001 to 0.1 (71). Such enhancements occur in very cold gas ($T \sim 10$ K), where differences in zero-point energies between competing isotopes become significant. They also occur in $^{12}C/^{13}C$ ratios, with enhancement in ^{13}C, but are most extreme for D (72, 73).

Downloaded from www.annualreviews.org. Guest (guest) IP: 174.18.91.56 On: Fri, 09 May 2025 21:45:19

4. THE IMPORTANT ROLE OF LABORATORY SPECTROSCOPY

Approximately 90% of all known interstellar molecules have been identified on the basis of their gas-phase rotational spectra, as opposed to ro-vibrational or electronic transitions. As discussed above, the temperatures in molecular gas are cold and favor the population of rotational levels. Furthermore, radio and millimeter-wave telescopes typically employ heterodyne mixing techniques to obtain spectral-line data, coupled with a multiplexing spectrometer as the back end. Such an instrument combination produces high spectral resolution, typically 1 part in 10^6–10^8. The other wavelength bands utilize CCD arrays and echelle spectrographs, which at best have resolutions of 1 part in 10^5 (74).

Lower-resolution spectra are also measured in the IR to examine dust grain composition (43). They are used to identify types of bonds in grains (e.g., aromatic C-C bends, Si-O stretch) rather than discrete molecules. For example, an 11-μm broad spectral feature has been observed in many circumstellar shells, arising from the Si-C stretch in SiC. SiC has many crystalline forms (75), and the feature is not specific to any single polytype. Rather, it serves as an overall indicator of SiC dust grains.

Rotational spectroscopy therefore is the major laboratory activity in support of astrochemistry. There are two typical methods employed to measure rotational spectra of potential interstellar molecules: (*a*) millimeter/submillimeter/THz direct absorption spectroscopy and (*b*) Fourier transform microwave/millimeter-wave cavity methods. These are not the only techniques; laser magnetic resonance has also been used for rotational measurements in the THz and far-IR (76). This latter method uses the Zeeman effect to tune molecular transitions into resonance with a fixed-frequency far-IR laser source. Therefore, obtaining zero-field rotational transitions requires extrapolation with a Zeeman Hamiltonian. Chirp-pulse Fourier transform systems are additionally employed (77) but do not have the sensitivity needed to detect many transient species.

Millimeter/submillimeter/THz direct absorption spectroscopy, which usually operates in the millimeter to THz frequencies (~65–1,500 GHz), is in principle a relatively straightforward process in which radiation is focused through a gas cell and into an incoherent detector. The change in power level due to a molecular absorption transition is measured (78, 79). In the past, lower-frequency systems have been commercially available, but most modern direct absorption instruments operate higher in frequency and are custom built in a given laboratory. Such spectrometers consist of three basic parts: a radiation source, a reaction chamber, and a detector. Typical radiation sources are Gunn oscillators, which provide frequency coverage up to ~150 GHz at 10–100 mW of power. They are phase locked for frequency stabilization. To obtain higher frequencies, the Gunn oscillators are used as input signals to Schottky diode multipliers, which double, triple, quadruple, and even quintuple the radiation with microwatts to a few milliwatts of power. The power decreases with multiplier harmonic, such that multiplier/amplifier chains are used at frequencies $\geq$1 THz. Reaction cells are typically constructed of glass or stainless steel, often employing a double-pass scheme with Gaussian-beam optics (80) for maximum sensitivity. Typical detectors for these spectrometers are InSb hot-electron bolometers. Some type of phase-sensitive detection, including FM or AM source or Stark or Zeeman molecule modulation, is used with these systems. Plasma discharges, Broida-type ovens, and other synthetic methods are employed to create the transient molecules often studied with these spectrometers.

Modeled after the more familiar nuclear magnetic resonance methods, the technique of pulsed-nozzle Fourier transform microwave spectroscopy in a Fabry-Pérot cavity was pioneered by Balle & Flygare (81) in 1981. This technique exploits the relatively short polarization time of rotational transitions of molecules relative to their relaxation, which results in the production of a relatively large electric field in the cavity compared to the background noise of the

Downloaded from www.annualreviews.org. Guest (guest) IP: 174.18.91.56 On: Fri, 09 May 2025 21:45:19

system, even with only a modest number density. Such systems typically consist of a large vacuum chamber containing two highly accurate spherical mirrors set in a near-confocal arrangement, which compose the Fabry-Pérot cavity. A frequency synthesizer is the radiation source, usually operated in the range of 4–20 GHz and as high as 40 GHz and whose output is coupled into and out of the cavity by quarter-wave antennas imbedded in each (or even one) mirror. Cavities vary but typically have an instantaneous bandwidth of ~1 MHz, resulting in an overall Q factor of approximately 10^4 to 10^5 over 4–40 GHz. The mirror distance is adjusted to optimize the Q for a given frequency. A short pulse of radiation (~1 μs) from the synthesizer is injected into the cavity for a given measurement. The synthesizer is stepped along in frequency for scanning, which can be done automatically under computer control. Higher-frequency operation (~40–90 GHz) requires more accurate mirrors, and the antennas are replaced by waveguide. Multipliers are needed to attain the higher frequencies, which require another set of low-noise amplifiers. More experimental details can be found in References 82–84.

The molecules to be studied enter the cavity via a supersonic beam created in a pulsed nozzle. The nozzle can be imbedded in the cavity mirrors, can be arranged perpendicular to the optical axis, or can be oriented through an angled port (see References 82–84). A single measurement lasts approximately 2,000 μs. The nozzle valve ejects a mixture of precursor/carrier gases (or the molecule candidate itself in a diluted sample) into the cavity. For molecule syntheses, an applied DC discharge, possibly with a laser ablation source, can be used to create the species of interest. A pulse of microwave radiation is injected shortly thereafter into the cavity, which sustains the energy. If one or more molecular transitions are resonant with the radiation in the cavity, the molecules absorb the signal and then re-emit it as a function of time. This emission signal, the free-induction decay (FID), is recorded in the time domain. The frequency information is recovered by a subsequent fast Fourier transform of the FID.

Species production and spectral analysis are key factors in the spectroscopy of molecules of astrophysical interest. In the early years of astrochemistry, detections were chiefly made of stable, closed-shell molecules that had been studied in the early years of microwave spectroscopy, including H_2O, ammonia, and formaldehyde. The rotational spectrum of H_2O, for example, has measurements dating back to the late 1940s, and numerous additional studies have followed over the years (85). These early data led to the identification of H_2O in the ISM in 1969 (86). More recent spectroscopy work on closed-shell molecules has involved much larger, organic-type molecules such as *N*-methylformamide (CH_3NHCHO) (87); glycolaldehyde (CH_2OHCHO) (88); acetohydroxamic acid ($CH_3CONHOH$), an isomer of glycine (89); and methyl isocyanate (CH_3NCO) (90). Organophosphorus compounds, including species such as PH_2CN and CH_3PH_2, are another area of interest (91); these species, however, are unstable and require special synthesis. The spectra of such large molecules can be challenging to analyze. As asymmetric tops, they have many favorable rotational transitions, with further complications due to the presence of internal rotation and multiple conformers. Laboratory spectra illustrating such complexity are shown in **Figure 3**, which displays transitions of CH_3PH_2 (the $J = 19 \leftarrow 18$) and the *cis*-beta cyanovinyl radical.

Free radicals and molecular ions are common in the ISM, and a great deal of spectroscopic effort has focused on such species. They need to be generated under nonequilibrium conditions, involving plasma discharges, discharge electrodes attached to nozzles, sputtering methods, and others. Recent emphasis on C-bearing radicals has been on chain-type species (92, 93), benzene-like compounds (94), and simple organometallics (95, 96). Because many of these species have unpaired electrons, the spectral analysis is complicated by the presence of fine structure and, if the molecule has a nuclear spin, by significant hyperfine interactions. For a linear molecule in a

Downloaded from www.annualreviews.org. Guest (guest) IP: 174.18.91.56 On: Fri, 09 May 2025 21:45:19

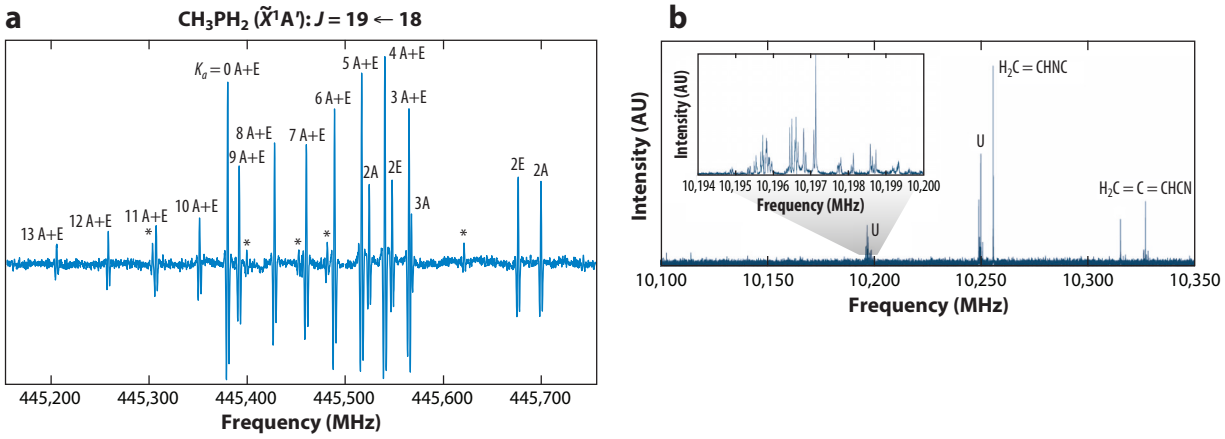

Figure 3

(*a*) Laboratory millimeter-wave spectrum of CH_3PH_2 ($\tilde{X}^1A'$). The $J = 19 \leftarrow 18$ rotational transition is split into asymmetry and internal rotation components, labeled by K_a, A, and E (91). Asterisks denote unidentified lines. (*b*) Fourier transform microwave spectra in a search for the *cis*-beta cyanovinyl radical, shown in the inset. U denotes unidentified lines. Panel *a* adapted from Reference 91. Panel *b* provided by K. Crabtree.

$^4\Delta$ electronic state, for example, with one nuclear spin (FeCN), the following Hamiltonian is needed to model the measured rotational transitions (97, 98):

$$\mathbf{H_{eff}} = \mathbf{H_{rot}} + \mathbf{H_{so}} + \mathbf{H_{ss}} + \mathbf{H_{mhf}} + \mathbf{H_{eqQ}} + \mathbf{H_{LD}}.$$

In addition to rotational motion, the electron spin-orbit, electron spin-spin, magnetic hyperfine, electric quadrupole, and lambda-doubling interactions must be considered. Higher-order spin terms are sometimes required as well. FeCN is the first Fe-bearing molecule detected in the ISM (26). The presence of a molecule in the gas phase with an Fe-C bond has prebiotic implications.

Spectroscopy in the IR and in the visible has also led to interstellar identifications. Important techniques are Fourier transform infrared spectroscopy (99) and laser-induced fluorescence (100). These methods have led to the identification of various interstellar molecules, such as C_3 (101) and VO (25). Experimental details can be found in Reference 102.

5. CARBON CHEMISTRY: THE FOCUS

Approximately 90% of all known gas-phase interstellar molecules contain C. This result is remarkable, given that C < O in the ISM and C should be principally in CO. Observations have shown that CO is widely distributed throughout the Galaxy and in many external galaxies (103, 104). Yet, C-bearing organic molecules constitute most of the chemical content of molecular clouds. Simple C-bearing molecules such as HCN, HNC, and CS are found in O-rich circumstellar envelopes as well (105). As discussed above, the preservation of C-C bonds may occur in circumstellar envelopes of C stars. Such preservation has been ignored because it was thought that the molecular content of AGB envelopes was destroyed in the PNe phase (47). It has now been shown that molecular material is preserved in PNe and then passed on to diffuse clouds (48–50). The wide range of polyatomic molecules now identified in diffuse clouds is evidence for this scenario (52, 53). Therefore, C-bearing molecules in circumstellar environments, as well as molecular clouds, must be considered in an integrated picture.

Downloaded from www.annualreviews.org. Guest (guest) IP: 174.18.91.56 On: Fri, 09 May 2025 21:45:19

5.1. Small Carbon-Bearing Molecules of Prebiotic Interest

The prebiotic nature of astrochemistry is illustrated in the small molecules found in the gas phase in the ISM. HCN, H_2CO, and NH_3 are common in molecular clouds. They could in principle compose the basis of a gas-phase Strecker synthesis, leading to the simplest amino acid, glycine (106). Despite numerous searches, glycine has never been detected in the ISM (88, 107). However, simple molecules with peptide bonds, including formamide (NH_2CHO) and acetamide (NH_2COCH_3), have been observed in dense clouds (11, 12, 108). Observations indicate that the two molecules are found in the same gas of the SgrB2(N) cloud, with an abundance ratio of $NH_2COCH_3/NH_2CHO \sim 1/3$. These findings suggest that NH_2CHO is the precursor to NH_2COCH_3 through a series of radiative association processes.

A simple, two-carbon sugar, glycolaldehyde, has been identified as well (12). Originally detected in SgrB2(N), this molecule has now been found in other molecular clouds, including regions of young star formation (109). The five-carbon sugar ribose is an essential component of DNA. Ribose is generated in the formose reaction, which converts formaldehyde by a 1 + 1 carbon addition to glycolaldehyde (110). Successive additions of H_2CO lead to ribose. It is notable that H_2CO is widespread in molecular clouds. An ion-molecule formose reaction scheme involving H_2COH^+ could lead to the diose. H_2COH^+ has been identified in SgrB2 and other molecular clouds (111). Other pathways to glycolaldehyde from H_2CO have also been examined theoretically (112).

A series of alcohols, amines, acids, aldehydes, and ketones add to the interstellar prebiotic mix (113, 114); see **Figure 4**. Other species present in clouds are methanimine (CH_2NH) and methylamine (CH_3NH_2), thought to be precursors to amino acids (10). In many cases, the formation mechanisms for the larger molecules are a mystery. Dimethyl ether (CH_3OCH_3), for example, is one of the most common complex organic species and has been a known interstellar molecule for decades. Although gas-grain reactions are often employed to explain molecule formation, for instance, CH_3OH (115), DFT calculations suggest a gas-phase route for CH_3OCH_3 (116). The major step for C-O-C bond formation is $CH_3OH + CH_3OH_2^+$, leading to $(CH_3)_2OH^+ + H_2O$, as shown in **Figure 5**. Reaction of the adduct ion with NH_3 results in the desired product.

These organic species are typically absent from the envelopes of C-rich stars. The carbon in these objects is chiefly contained in a series of acetylenic-type molecules, including the hydrocarbon series C_2H, C_3H, C_4H, C_5H, etc., and in species with a terminal N or S atom, such as CCN, C_3N, C_5N, C_3N^-, C_5N^-, C_3S, C_4S, and others (117, 118). However, H_2CO is present in the envelope of IRC+10216, as are CH_2NH and CH_3CN (35). Larger molecules such as ethanol or dimethyl ether are not observed in these objects. They are also not present in O-rich envelopes such as that of VY CMa (35).

5.2. Larger Carbon Structures

The discovery of the fullerenes C_{60}, C_{70}, and possibly C_{60}^+ in interstellar gas suggests the presence of larger C-bearing structures in the ISM. Both C_{60} and C_{70} have been identified in PNe

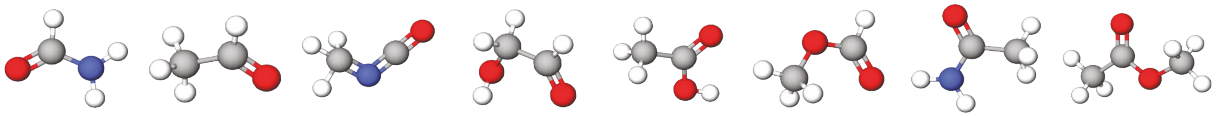

Figure 4

Representative complex organic molecules found in molecular clouds with star formation.

Downloaded from www.annualreviews.org. Guest (guest) IP: 174.18.91.56 On: Fri, 09 May 2025 21:45:19

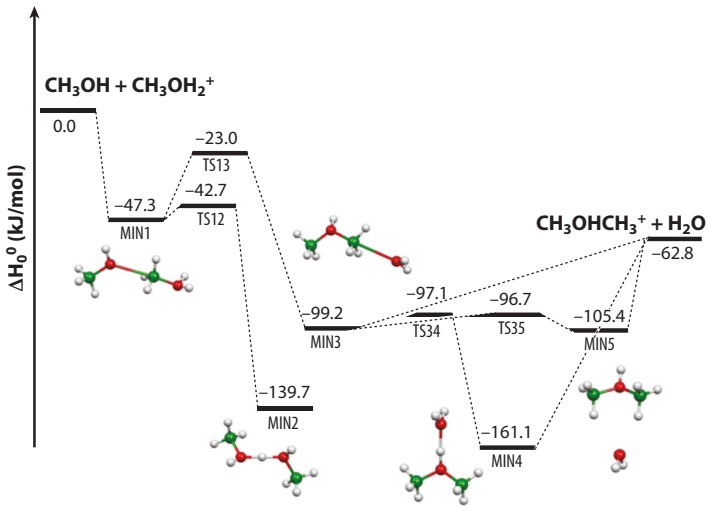

Figure 5

Gas-phase reaction pathway leading from CH_3OH to CH_3OCH_3, predicted by DFT calculations and experiment. The final ion, $CH_3OHCH_3^+$, then reacts with ammonia to lead to neutral dimethyl ether. Figure adapted from Reference 116.

and other circumstellar environments, as well as in diffuse clouds on the basis of four major IR features at 7.0, 8.5, 17.4, and 18.9 μm (68). C_{60}^+ appears in diffuse clouds, accounting for several diffuse interstellar bands (DIBs) (14), and possibly in some sources where the neutral fullerenes are observed (68). The DIBs have been a long-standing problem in astronomy and have defied identification for decades (52, 119). The C_{60}^+ assignment is based on lab measurement of the molecule attached to a He atom. Despite the success of spectral identifications, the formation mechanism for the fullerenes has been a puzzle. It is difficult to conceive a facile process that can bring together 60 sp^2-hybridized C atoms in environments that are very rich in H and other elements such as O and N under typical astrophysical conditions. Formation from atoms, the so-called bottom-up pathway, is not likely, as formation timescales are too long given typical interstellar densities and temperatures. Top-down synthesis from larger C structures, either hydrogenated amorphous carbon or polycyclic aromatic hydrocarbons, has been suggested (120, 121). However, there are difficulties in the intermediate steps, such as the elimination of hydrogen atoms in an H-rich gas and the rearrangement of bonds into a closed carbon cage (122). Furthermore, UV radiation is often required for these processes, and some sources of C_{60}, such as IRAS 06338, are too cool to be substantial UV emitters (123).

Recently, a new formation mechanism was proposed for interstellar fullerenes: shock processing of circumstellar SiC grains. This hypothesis is based on laboratory experiments with analog grains using transmission electron microscopy (TEM) (75, 124). In these experiments, SiC grains with the 3C cubic structure—the most common form of circumstellar SiC dust—were rapidly heated under vacuum to ~1,300 K, simulating a shock wave in a circumstellar envelope. Such shocks are present in circumstellar gas and can originate with stellar pulsations associated with mass loss events (125). The fast rise in temperature leaches the Si atoms from the grain surface, creating graphitic sheets. The creation of graphite sheets from SiC has been known for decades in the materials science community (126), although under somewhat different conditions. Surface defects in the SiC crystal then distort the six-membered rings characteristic of graphite, creating a forest of hemispherical structures observed with TEM. These features have both the

Downloaded from www.annualreviews.org. Guest (guest) IP: 174.18.91.56 On: Fri, 09 May 2025 21:45:19

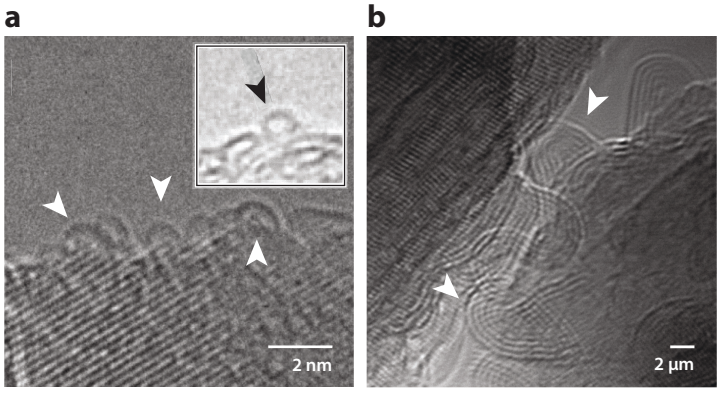

Figure 6

(*a*) Transmission electron microscope (TEM) image of a shock-heated SiC sample grain with fullerene-sized hemispheres lining the surface (*white arrowheads*). (*Inset*) State-of-the-art TEM image of C_{60} (*black arrowhead*). (*b*) TEM image of carbon nanotubes growing on the SiC grain surface, indicated by white arrows. Figure reproduced with permission from Reference 124.

five- and six-membered rings necessary for C_{60} and match its diameter of ~1 nm. To the limit of the measurement techniques, these features are C_{60} but are still attached to the graphite surface; see **Figure 6**. The striations (**Figure 6**) under the C_{60} features are the SiC lattice. The inset of **Figure 6** shows a representative TEM image of C_{60} obtained under very favorable conditions (127). The C_{60} images are comparable, illustrating the difficulty in detecting individual fullerene molecules with TEM. The experiments also showed that subsequent heating of the grains generated multiwalled carbon nanotubes (CNTs) on the surface as well (124), also shown in **Figure 6**.

These results suggest that shock heating of SiC grains in circumstellar gas produces the observed interstellar fullerenes, even in an H-rich situation. Furthermore, the process can also lead to nanotube formation. These CNTs may be another carrier of the DIBs (128). The fullerenes and CNTs are then ejected into the diffuse ISM with stellar mass loss. This scenario also explains the absence of SiC grains in the ISM, a current mystery (129), as they are disguised by a graphite coating. In fact, presolar grains have been found with SiC cores surrounded by graphite layers (75).

Carbon is also contained in dust grains, the most important forms being SiC and amorphous C (129). They are potentially additional sources of C. Shocks in star-forming regions may disrupt these grains, releasing gas-phase carbon for molecular synthesis (36).

6. WHERE IS THE PHOSPHORUS IN THE GALAXY?

Phosphorus is a key ingredient for biochemistry and the origin of life, playing a major role in replication, metabolism, and cellular structure. For example, phosphate esters create the backbone of DNA and RNA. The widespread presence in the Earth's current biosphere of RNA catalysts and cofactors suggests that RNA was indeed the first biopolymer (130). Furthermore, ATP (adenosine triphosphate) is the key molecule in the cell energy cycle, containing three phosphate ester groups. P is also found in phospholipids, the main structural component of cellular membranes in living systems, and even in bone as mineral phosphates, for example, apatite [$Ca_5(PO_4)_3(OH, F, Cl)$] (131).

In addition to being represented in living systems on Earth, P is common in the Solar System, as either phosphate (PO_4^{3-} bonded with Ca^{2+}, Mg^{2+}, etc.) or phosphide [schreibersite, or

Downloaded from www.annualreviews.org. Guest (guest) IP: 174.18.91.56 On: Fri, 09 May 2025 21:45:19

(Fe, Ni)$_3$P] (132, 133). Schreibersite and the phosphate apatite are frequently found in meteorites, including carbonaceous chondrites (133). Furthermore, it has been hypothesized that P, alloyed with the pure metals Fe and Ni as phosphides, may have served as nucleation material for planetary cores (132).

In the ISM, P has been a mystery. The atomic transitions of this element and P^+ are in unfavorable regions of the electromagnetic spectrum, either in the near-IR region or in the UV, where they are obscured by atmospheric features (134). Space-born observations of atomic P using FUSE and Copernicus satellites have enabled better measurements, but only within a few kiloparsecs (where 1 kpc = 3.086×10^{16} km = 3,261 light years) of the solar neighborhood (134).

Molecules containing P have provided a separate avenue to study its distribution in the Galaxy, as well as to evaluate its prebiotic role. Searches, however, have been limited by laboratory spectroscopic measurements of P-bearing species. The first detection of an interstellar P-bearing species was in 1987, when PN was discovered in the Orion-KL region of the Orion Molecular Cloud (135). PN was subsequently observed in additional molecular clouds throughout the next few decades (136). More recently, the biologically relevant PO has been identified in a series of clouds, including the star-forming regions Orion-KL, W51 1e/2e, W3(OH), and L1157 and the low-mass protostar B1 (136–138), along with PN. These two species have even been identified in clouds at the outskirts of the Galaxy (134).

In contrast, circumstellar envelopes of evolved stars appear to have a more diverse, if limited, P chemistry. The first P-bearing molecule identified in a circumstellar envelope was CP, found in the C-rich shell of IRC+10216 (139). This discovery was followed by the detections over several decades of PN, CCP, HCP, PH_3, and SiP, mostly in IRC+10216 (140, 141). PH_3, PN, and HCP were also observed in the very young protoplanetary nebula CRL2688 (142). PO was first identified as an interstellar molecule in the O-rich envelope of the hypergiant VY CMa (143) and years later was found in molecular clouds (136–138). PO has now been observed in other O-rich envelopes, such as those of NML Cyg, IK Tau, and R Cas, also in the presence of PN (144). The observation of PO is particularly interesting, as this was the first molecule (and thus far the only one) observed in space with a P-O bond. It is remarkable that PN and PO almost always coexist, suggesting a related synthesis (136).

Table 2 provides a summary of interstellar P compounds. A total of seven P-bearing species have been securely identified in the ISM. The most abundant and widely observed species is PO, which is found in O-rich envelopes and in molecular clouds, as discussed above. Its abundance in circumstellar shells is as high as $\sim 10^{-7}$, which means that approximately 30% of the available P is in the form of PO. In molecular clouds, the abundance is significantly lower at $f \sim 10^{-10}$. Of interest is that no true organophosphorus molecules have been discovered in the ISM, even though the N analogs are abundant. For example, CH_3NH_2 is a well-known interstellar molecule, but searches for CH_3PH_2 have proven unsuccessful (91).

7. PREBIOTIC MOLECULES AND THE GALACTIC HABITABLE ZONE

There are currently more than 5,000 known exoplanets (145). The question then arises: Which could be habitable? To this aim, the concept of the galactic habitable zone (GHZ) has been conceived. The GHZ is the section in a galaxy where conditions are suitable for the long-term survival of living systems on planets (146). Among the numerous factors that define the GHZ are higher metallicity for planet formation; the absence of catastrophic events such as SNe explosions; and even lithopanspermia, the transport of rocks containing microorganisms from one planet to other stellar systems (147, 148). In the Galaxy, these considerations have placed the GHZ in an annular disk with varied distances from the Galactic Center (R_{GC}), including the Solar System; others have proposed that the entire disk is suitable (149).

Downloaded from www.annualreviews.org. Guest (guest) IP: 174.18.91.56 On: Fri, 09 May 2025 21:45:19

The presence of prebiotic molecules in dense molecular clouds has also been proposed to constrain the GHZ (149). These clouds are located throughout the Galaxy, on the basis of CO observations (104), providing an extended sample. Furthermore, life will probably not survive in regions too hostile for the existence of organic compounds.

Recent observations of prebiotic molecules have focused on the so-called Galactic Edge Clouds, located in the Outer Galaxy at $R_{GC} \sim 12.9$–23.5 kpc. In these clouds, organic molecules, including H_2CO, CH_3OH, and CH_3CCH, have been found (149, 150). Very recently, PO and PN were also detected in one cloud near $R_{GC} \sim 23$ kpc (134). Therefore, all the NCHOPS elements (21) are present in molecules at the edge of the Galaxy. Furthermore, the abundance of CH_3OH does not appear to decrease significantly with distance from R_{GC}, even at $R_{GC} \sim 20$–23 kpc (149). It is thought that the C abundance and star formation rate steadily decline with R_{GC} (149). The production of methanol must then be extremely efficient in the Edge Clouds. These data suggest that the GHZ extends as far as $R_{GC} \sim 23$ kpc and that exoplanets that can support life may exist in the Outer Galaxy. Currently, all known exoplanets are near the Solar circle (145).

8. CONCLUSIONS

An important outcome for astrochemistry has been the recognition of its possible role in the origin of life and its connection to the formation of solar systems. The presence of gas-phase organic molecules throughout the Galaxy in extremely large quantities, and their survival under harsh conditions, is suggestive that this molecular material may provide the foundation for a far richer biochemical synthesis on planetary surfaces. Furthermore, the ejecta of carbon stars may have provided the C enrichment needed to overcome the obstacles of the O-rich ISM, delivering the seeds for organic chemistry. Another NCHOPS element, phosphorus, is being found more frequently in molecules across the Galaxy, even at the Galactic Edge. From the standpoint of Earth, exogenous delivery likely provided important starting materials for early life, bringing more usable molecular material than what had resided in the crust. Further investigations into the role of prebiotic astrochemistry, with new telescopes like the James Webb Space Telescope, will challenge researchers for decades to come.

DISCLOSURE STATEMENT

The author is not aware of any affiliations, memberships, funding, or financial holdings that might be perceived as affecting the objectivity of this review.

ACKNOWLEDGMENTS

This article was based on research supported by NSF grants AST-1907910 and AST-2307305 and NASA grant 80NSSC18K0584 (Emerging Worlds).

LITERATURE CITED

1. Douglas AE, Herzberg GH. 1941. Note on CH^+ in interstellar space and in the laboratory. *Astrophys. J.* 94:381
2. Townes CH, Schawlow A. 1971. *Microwave Spectroscopy*. New York: Dover
3. Cheung AC, Rank DM, Townes CH, Thornton DD, Welch WJ. 1968. Detection of NH_3 molecules in the interstellar medium by their microwave emission. *Phys. Rev. Lett.* 21:1701
4. Weinreb S, Barrett AH, Meeks ML, Henry JC. 1963. Radio observations of OH in the interstellar medium. *Nature* 200:829–31
5. Snyder LE, Buhl D, Zuckerman B, Palmer P. 1969. Microwave detection of interstellar formaldehyde. *Phys. Rev. Lett.* 22:679–81

Downloaded from www.annualreviews.org. Guest (guest) IP: 174.18.91.56 On: Fri, 09 May 2025 21:45:19

6. Wilson RW, Jefferts KB, Penzias AA. 1970. Carbon monoxide in the Orion Nebula. *Astrophys. J.* 161:L43–44
7. Snyder LE, Buhl D. 1971. Observations of radio emission from interstellar hydrogen cyanide. *Astrophys. J.* 163:L47–52
8. Wilson RW, Penzias AA, Jefferts KB, Kutner M, Thaddeus P. 1971. Discovery of interstellar silicon monoxide. *Astrophys. J.* 167:L97–100
9. Thaddeus P, Kutner ML, Penzias AA, Wilson RW, Jefferts KB. 1972. Interstellar hydrogen sulfide. *Astrophys. J.* 176:L73–76
10. Halfen DT, Ilyushin VV, Ziurys LM. 2013. Insights into surface hydrogenation in the interstellar medium: observations of methanimine and methyl amine in Sgr B2(N). *Astrophys. J.* 767:66
11. Hollis JM, Lovas FJ, Remijan AJ, Jewell PR, Ilyushin VV, Kleiner I. 2006. Detection of acetamide (CH_3CONH_2): the largest interstellar molecule with a peptide bond. *Astrophys. J.* 643:L25–28
12. Halfen DT, Apponi AJ, Woolf NJ, Polt R, Ziurys LM. 2006. A systematic study of glycolaldehyde in Sgr B2(N) at 2 and 3 millimeters: criteria for detecting large interstellar molecules. *Astrophys. J.* 639:237–45
13. Cami J, Bernard-Salas J, Peeters E, Malek SE. 2010. Detection of C_{60} and C_{70} in a young planetary nebula. *Science* 329:1180–82
14. Campbell EK, Holz M, Gerlich D, Maier JP. 2015. Laboratory confirmation of C_{60}^+ as the carrier of two diffuse interstellar bands. *Nature* 523:322–23
15. Johansson LE, Anderson C, Elldér J, Friberg P, Hjalmarson Å, et al. 1985. The spectra of Orion A and IRC+10216 between 72.2 and 91.1 GHz. *Astron. Astrophys. Suppl. Ser.* 60:135–68
16. Keady JJ, Ridgway ST. 1993. The IRC+10216 circumstellar envelope. III. Infrared molecular line profiles. *Astrophys. J.* 406:199–214
17. Goldhaber DM, Betz AL. 1984. Silane in IRC+10216. *Astrophys. J.* 579:L55–58
18. Wilson TL, Rohlfs K, Hüttemeister S. 2009. *Tools of Radio Astronomy*. Berlin: Springer
19. Meyer DM, Roth KC. 1991. Discovery of interstellar NH. *Astrophys. J.* 376:L49–52
20. Hunaerts J. 1967. C_2 Ballick-Ramsay bands in late carbon stars. *Astrophys. J.* 149:L31–32
21. Forgan D, Dayal P, Cockell C, Libeskind N. 2017. Evaluating galactic habitability using high-resolution cosmological simulations of galaxy formation. *Int. J. Astrobiol.* 16:60–73
22. Ziurys LM. 2019. Interstellar molecules and their prebiotic potential. In *Handbook of Astrobiology*, ed. VM Kolb, pp. 168–85. Boca Raton, FL: CRC Press
23. Neufeld DA, Schilke P, Menten KM, Wolfire MG, Black JH, et al. 2006. Discovery of interstellar CF^+. *Astron. Astrophys.* 454:L37–40
24. Cernicharo J, Cabezas C, Pardo JR, Agúndez M, Roncero O, et al. 2023. The magnesium paradigm in IRC+10216: discovery of MgC_4H^+, MgC_3N^+, MgC_6H^+, and MgC_5N^+. *Astron. Astrophys.* 672:L13
25. Humphreys RM, Ziurys LM, Bernal JJ, Gordon MS, Helton LA, et al. 2019. The unexpected spectrum of the innermost ejecta of the red hypergiant VY CMa. *Astrophys. J. Lett.* 874:L26
26. Zack LN, Halfen DT, Ziurys LM. 2011. Detection of FeCN ($X^4\Delta_i$) in IRC+10216: a new interstellar molecule. *Astrophys. J. Lett.* 733:L36
27. Schilke P, Neufeld DA, Müller HS, Comito C, Bergin EA, et al. 2014. Ubiquitous argonium (ArH^+) in the diffuse interstellar medium: a molecular tracer of almost purely atomic gas. *Astron. Astrophys.* 566:A29
28. Green DA. 2015. Constraints on the distribution of supernova remnants with Galactocentric radius. *Mon. Not. R. Astron. Soc.* 454:1517–24
29. Dorschner J, Henning T. 1995. Dust metamorphosis in the galaxy. *Astron. Astrophys. Rev.* 6:271–333
30. Koo BC, Lee YH, Moon DS, Yoon SC, Raymond JC. 2013. Phosphorus in the young supernova remnant Cassiopeia A. *Science* 342:1346–48
31. Smartt SJ. 2009. Progenitors of core-collapse supernovae. *Annu. Rev. Astron. Astrophys.* 47:63–106
32. Milam SN, Woolf NJ, Ziurys LM. 2009. Circumstellar $^{12}C/^{13}C$ isotope ratios from millimeter observations of CN and CO: mixing in carbon- and oxygen-rich stars. *Astrophys. J.* 690:837–49
33. Glassgold AE. 1996. Circumstellar photochemistry. *Annu. Rev. Astron. Astrophys.* 34:241–77
34. Cernicharo J, Guélin M, Kahane C. 2000. A λ2 mm molecular line survey of the C-star envelope IRC+10216. *Astron. Astrophys. Suppl. Ser.* 142:181–215

Downloaded from www.annualreviews.org. Guest (guest) IP: 174.18.91.56 On: Fri, 09 May 2025 21:45:19

35. Tenenbaum ED, Dodd JL, Milam SN, Woolf NJ, Ziurys LM. 2010. The Arizona Radio Observatory 1 mm spectral survey of IRC+10216 and VY Canis Majoris (215–285 GHz). *Astrophys. J. Suppl. Ser.* 190:348–417
36. Ziurys LM, Halfen DT, Geppert W, Aikawa Y. 2016. Following the interstellar history of carbon: from the interiors of stars to the surfaces of planets. *Astrobiology* 16:997–1012
37. Singh AP, Edwards JL, Humphreys RM, Ziurys LM. 2021. Molecules and outflows in NML Cygni: new insights from a 1 mm spectral line survey. *Astrophys. J. Lett.* 920:L38
38. Singh AP, Edwards JL, Ziurys LM. 2022. The Arizona Radio Observatory 1 mm spectral survey of the hypergiant star NML Cygni (215–285 GHz). *Astron. J.* 164:230
39. Humphreys RM, Helton LA, Jones TJ. 2007. The three-dimensional morphology of VY Canis Majoris. I. The kinematics of the ejecta. *Astron. J.* 133:2716–29
40. Tenenbaum ED, Dodd JL, Milam SN, Woolf NJ, Ziurys LM. 2010. Comparative spectra of oxygen-rich versus carbon-rich circumstellar shells: VY Canis Majoris and IRC+10216 at 215–215 GHz. *Astrophys. J. Lett.* 720:L102–7
41. Jones A. 2001. Dust in the dense interstellar medium. In *From Darkness to Light* (ASP Conference Series, Vol. 243), ed. T Montmerle, P André, pp. 37–46. San Francisco: Astron. Soc. Pac.
42. Lodders K, Fegley B. 1999. Condensation chemistry of circumstellar grains. *Proc. Int. Astron. Union* 191:279–90
43. Kwok S. 2004. The synthesis of organic and inorganic compounds in evolved stars. *Nature* 430:985–91
44. Lodders K, Amari S. 2005. Presolar grains from meteorites: remnants from the early times of the solar system. *Geochemistry* 65:93–166
45. Gobrecht D, Cherchneff I, Sarangi A, Plane JMC, Bromley ST. 2016. Dust formation in the oxygen-rich AGB star IK Tauri. *Astron. Astrophys.* 585:A6
46. Kwok S. 2000. *The Origin and Evolution of Planetary Nebulae*. New York: Cambridge Univ. Press
47. Redman MP, Viti S, Cau P, Williams DA. 2003. Chemistry and clumpiness in planetary nebulae. *Mon. Not. R. Astron. Soc.* 345:1291–96
48. Schmidt DR, Ziurys LM. 2016. Hidden molecules in planetary nebulae: new detections of HCN and HCO^+ from a multi-object survey. *Astrophys. J.* 817:175
49. Schmidt DR, Zack LN, Ziurys LM. 2018. Widespread CCH and c-C_3H_2 in the Helix Nebula: unraveling the chemical history of hydrocarbons. *Astrophys. J. Lett.* 864:L31
50. Schmidt DR, Gold KR, Sinclair A, Bergstrom S, Ziurys LM. 2022. HCN and HCO^+ in planetary nebulae: the next level. *Astrophys. J.* 927:46
51. Bianchi S, Schneider R. 2007. Dust formation and survival in supernova ejecta. *Mon. Not. R. Astron. Soc.* 378:973–82
52. Snow TP, McCall BJ. 2006. Diffuse atomic and molecular clouds. *Annu. Rev. Astron. Astrophys.* 44:367–414
53. Liszt HS, Lucas R, Pety J. 2006. Comparative chemistry in diffuse clouds. V. Ammonia and formaldehyde. *Astron. Astrophys.* 448:253–59
54. Lee J-E, Bergin EA, Evans NJ II. 2004. Evolution of chemistry and molecular line profiles during protostellar collapse. *Astrophys. J.* 617:360–83
55. Nummelin A, Bergman P, Hjalmarson Å, Friberg P, Irvine WM, et al. 2000. A three-position spectral line survey of Sagittarius B2 between 218 and 263 GHz. II. Data analysis. *Astrophys. J. Suppl. Ser.* 128:213–43
56. Bruenken S, Gupta H, Gottleib CA, McCarthy MC, Thaddeus P. 2007. Detection of the carbon chain negative ion C_8H^- in TMC-1. *Astrophys. J. Lett.* 664:L43–46
57. Hatchell J, Thompson MA, Millar TJ, Macdonald GH. 1998. Sulphur chemistry and evolution in hot cores. *Astron. Astrophys.* 338:713–22
58. Wright MCH, Plambeck RL. 2017. ALMA images of the Orion hot core at 349 GHz. *Astrophys. J.* 843:83
59. Vidal THG, Wakelam V. 2018. A new look at sulphur chemistry in hot cores and corinos. *Mon. Not. R. Astron. Soc.* 474:5575–87
60. Öberg KI, Bergin EA. 2021. Astrochemistry and compositions of planetary systems. *Phys. Rep.* 893:1–48
61. Eistrup C, Walsh C, van Dishoeck EF. 2018. Molecular abundances and C/O ratios in chemically evolving planet-forming disk midplanes. *Astron. Astrophys.* 613:A14

Downloaded from www.annualreviews.org. Guest (guest) IP: 174.18.91.56 On: Fri, 09 May 2025 21:45:19

62. Booth RA, Ilee JD. 2019. Planet-forming material in a protoplanetary disc: the interplay between chemical evolution and pebble drift. *Mon. Not. R. Astron. Soc.* 487:3998–4011
63. Cevallos Soto A, Tan JC, Hu X, Hsu CJ, Walsh C. 2022. Inside-out planet formation. VII. Astrochemical models of protoplanetary discs and implications for planetary compositions. *Mon. Not. R. Astron. Soc.* 517:2285–308
64. Mulders GD, Pascucci I, Apai D, Ciesla FJ. 2018. The Exoplanet Population Observation Simulator. I. The inner edges of planetary systems. *Astrophys. J.* 156:24
65. Voosen P. 2019. Project traces 500 million years of roller-coaster climate. *Science* 364:716–17
66. Denlinger MC. 2005. The origin and evolution of the atmospheres of Venus, Earth, and Mars. *Earth Moon Planets* 96:59–80
67. Morbidelli A, Nesvorny D, Laurenz V, Marchi S, Rubie DC, et al. 2017. *The lunar late heavy bombardment as a tail-end of planet accretion*. Presented at Lunar Planet. Sci. Conf., 48th, Contrib. 1964, ID 2298, Woodslands, Tex., Mar. 20–24
68. Zhang Y, Kwok S, Sadjadi S. 2016. Fullerenes and fulleranes in circumstellar envelopes. *J. Phys. Conf. Ser.* 728:052004
69. Pizzarello S. 2007. Question 2: why astrobiology? *Orig. Life Evol. Biosph.* 37:341–44
70. Busemann H, Young AF, Alexander CM, Hoppe P, Mukhopadhyay S, Nittler LR. 2006. Interstellar chemistry recorded in organic matter from primitive meteorites. *Science* 312:727–30
71. Caselli P, Ceccarelli C. 2012. Our astrochemical heritage. *Astron. Astrophys. Rev.* 20:56
72. Millar TJ, Bennett A, Herbst E. 1989. Deuterium fractionation in dense interstellar clouds. *Astrophys. J.* 340:906–20
73. Halfen DT, Woolf NJ, Ziurys LM. 2017. The $^{12}C/^{13}C$ ratio in Sgr B2 (N): constraints for galactic chemical evolution and isotopic chemistry. *Astrophys. J.* 845:158
74. Pfeiffer MJ, Frank C, Baumüller D, Fuhrmann K, Gehren T. 1998. FOCES—a fibre optics Cassegrain echelle spectrograph. *Astron. Astrophys. Suppl. Ser.* 130:381–93
75. Bernal JJ, Haenecour P, Howe J, Zega TJ, Amari S, Ziurys LM. 2019. Formation of interstellar C_{60} from silicon carbide circumstellar grains. *Astrophys. J. Lett.* 883:L43
76. Brown JM, Körsgen H, Beaton SP, Evenson KM. 2006. The rotational and fine-structure spectrum of FeH, studied by far-infrared laser magnetic resonance. *J. Chem. Phys.* 124:234309
77. Prozument K, Park GB, Shaver RG, Vasiliou AK, Oldham JM, et al. 2014. Chirped-pulse millimeter-wave spectroscopy for dynamics and kinetics studies of pyrolysis reactions. *Phys. Chem. Chem. Phys.* 16:15739–51
78. Hirota E. 1985. *High-Resolution Spectroscopy of Transient Molecules*. Berlin/Heidelberg, Ger.: Springer
79. Ziurys LM, Barclay WL Jr., Anderson MA, Fletcher DA, Lamb JW. 1994. A millimeter/submillimeter spectrometer for high resolution studies of transient molecules. *Rev. Sci. Instrum.* 65:1517–22
80. Goldsmith PF. 1998. *Quasi-Optical Systems: Gaussian Beam Quasi-Optical Propagation and Applications*. Piscataway, NJ: IEEE
81. Balle TJ, Flygare WH. 1981. Fabry-Perot cavity pulsed Fourier transform microwave spectrometer with a pulsed nozzle particle source. *Rev. Sci. Instrum.* 52:33–45
82. Thorwirth S, McCarthy MC, Dudek JB, Thaddeus P. 2005. Fourier transform microwave spectroscopy of vinyldiacetylene, vinyltriacetylene, and vinylcyanodiacetylene. *J. Chem. Phys.* 122:184308
83. Xie F, Fusé M, Hazrah AS, Jäger W, Barone V, Xu Y. 2020. Discovering the elusive global minimum in a ternary chiral cluster: rotational spectra of propylene oxide trimer. *Angew. Chem. Int. Ed.* 59:22427–30
84. Sun M, Apponi AJ, Ziurys LM. 2009. Fourier transform microwave spectroscopy of HZnCN ($X\,^1\Sigma^+$) and ZnCN ($X\,^2\Sigma^+$). *J. Chem. Phys.* 130:034309
85. Yu S, Pearson JC, Drouin BJ, Martin-Drumel MA, Pirali O, et al. 2012. Measurement and analysis of new terahertz and far-infrared spectra of high temperature water. *J. Mol. Spectrosc.* 279:16–25
86. Cheung AC, Rank DM, Townes CH, Thornton DD, Welch WJ. 1969. Detection of water in interstellar regions by its microwave emission. *Nature* 221:626–28
87. Belloche A, Meshcheryakov AA, Garrod RT, Ilyushin VV, Alekseev EA, et al. 2017. Rotational spectroscopy, tentative interstellar detection, and chemical modeling of N-methylformamide. *Astron. Astrophys.* 601:A49

Downloaded from www.annualreviews.org. Guest (guest) IP: 174.18.91.56 On: Fri, 09 May 2025 21:45:19

88. Butler RA, De Lucia FC, Petkie DT, Møllendal H, Horn A, Herbst E. 2001. The millimeter-and submillimeter-wave spectrum of glycolaldehyde (CH_2OHCHO). *Astrophys. J. Suppl. Ser.* 134:319–21
89. Sanz-Novo M, Alonso JL, Rivilla VM, McGuire BA, León I, et al. 2022. Laboratory detection and astronomical study of interstellar acetohydroxamic acid, a glycine isomer. *Astron. Astrophys.* 666:A134
90. Halfen DT, Ilyushin VV, Ziurys LM. 2015. Interstellar detection of methyl isocyanate CH_3NCO in Sgr B2 (N): a link from molecular clouds to comets. *Astrophys. J. Lett.* 812:L5
91. Halfen DT, Clouthier DJ, Ziurys LM. 2014. Millimeter/submillimeter spectroscopy of PH_2CN (X^1A') and CH_3PH_2 (X^1A'): probing the complexity of interstellar phosphorus chemistry. *Astrophys. J.* 796:36
92. Gupta H, Bruenken S, Tamassia F, Gottlieb CA, McCarthy MC, Thaddeus P. 2007. Rotational spectra of the carbon chain negative ion C_4H^- and C_8H^-. *Astrophys. J. Lett.* 655:L57–60
93. McCarthy MC, Chen W, Apponi AJ, Gottlieb CA, Thaddeus P. 1999. Hyperfine structure of the C_5H, C_6H, and C_8H radicals. *Astrophys. J.* 520:158–61
94. Martinez O, Crabtree KN, Gottlieb CA, Stanton JF, McCarthy MC. 2014. An accurate molecular structure of phenyl, the simplest aryl radical. *Angew. Chem.* 127:1828–31
95. Halfen DT, Ziurys LM. 2018. The pure rotational spectrum of the T-shaped AlC_2 radical (X^2A_1). *Phys. Chem. Chem. Phys.* 20:11047–52
96. Changala PB, Gupta H, Cernicharo J, Pardo JR, Agúndez M, et al. 2022. Laboratory and astronomical discovery of magnesium dicarbide, MgC_2. *Astrophys. J. Lett.* 940:L42
97. Flory MA, Ziurys LM. 2011. Millimeter-wave rotational spectroscopy of FeCN ($X^4\Delta_i$) and FeNC ($X^6\Delta_i$): determining the lowest energy isomer. *J. Chem. Phys.* 135:184303
98. Zack LN, Min J, Harris BJ, Flory MA, Ziurys LM. 2011. Fourier-transform microwave spectroscopy of FeCN ($X^4\Delta_i$): confirmation of the quartet electronic ground state. *Chem. Phys. Lett.* 514:202–6
99. Hodges JN, Bernath PF. 2018. Fourier transform spectroscopy of the $C^3\Delta$–$X^3\Delta$ transition of TiO in support of exoplanet spectroscopy. *Astrophys. J.* 863:36
100. Jakubek ZJ, Nakhate SG, Simard B. 2002. The SiP molecule: first observation and spectroscopic characterization. *J. Chem. Phys.* 116:6513–20
101. Hinkle KW, Keady JJ, Bernath PF. 1988. Detection of C_3 in the circumstellar shell of IRC+10216. *Science* 241:1319–22
102. Bernath PF. 2020. *Spectra of Atoms and Molecules*. New York: Oxford Univ. Press
103. Young JS, Scoville N. 1982. Extragalactic CO-gas distributions which follow the light in IC 342 and NGC 6946. *Astrophys. J.* 258:467–89
104. Heyer M, Dame TM. 2015. Molecular clouds in the Milky Way. *Annu. Rev. Astron. Astrophys.* 53:583–629
105. Ziurys LM, Tenenbaum ED, Pulliam RL, Woolf NJ, Milam SN. 2009. Carbon chemistry in the envelope of VY Canis Majoris: implications for oxygen-rich evolved stars. *Astrophys. J.* 695:1604–13
106. Lerner NR, Peterson E, Chang S. 1993. The Strecker synthesis as a source of amino acids in carbonaceous chondrites: deuterium retention during synthesis. *Geochim. Cosmochim. Acta* 57:4713–23
107. Jiménez-Serra I, Martín-Pintado J, Rivilla VM, Rodríguez-Almeida L, Alonso ER, et al. 2020. Toward the RNA-world in the interstellar medium—detection of urea and search of 2-amino-oxazole and simple sugars. *Astrobiology* 20:1048–66
108. Ziurys LM, Adande GR, Edwards JL, Schmidt DR, Halfen DT, Woolf NJ. 2015. Prebiotic chemical evolution in the astrophysical context. *Orig. Life Evol. Biosph.* 45:275–88
109. De Simone M, Codella C, Testi L, Belloche A, Maury AJ, et al. 2017. Glycolaldehyde in Perseus young solar analogs. *Astron. Astrophys.* 599:A121
110. Breslow R. 1959. On the mechanism of the formose reaction. *Tetrahedron Lett.* 1:22–26
111. Ohishi M, Shin-ichi I, Amano T, Oka H, Irvine WM, et al. 1996. Detection of a new interstellar molecular ion, H_2COH^+ (protonated formaldehyde). *Astrophys. J.* 471:L61–64
112. Silva SG, Vichietti RM, Haiduke RL, Machado FB, Spada RF. 2020. Methanol and glycolaldehyde production from formaldehyde in massive star-forming regions. *Mon. Not. R. Astron. Soc.* 497:4486–94
113. Belloche A, Müller HSP, Garrod RT, Menten KM. 2016. Exploring molecular complexity with ALMA (EMoCA): deuterated complex organic molecules in Sagittarius B2(N2). *Astron. Astrophys.* 587:A91
114. Skouteris D, Balucani N, Ceccarelli C, Vazart F, Puzzarini C, et al. 2018. The genealogical tree of ethanol: gas-phase formation of glycolaldehyde, acetic acid, and formic acid. *Astrophys. J.* 854:135

Downloaded from www.annualreviews.org. Guest (guest) IP: 174.18.91.56 On: Fri, 09 May 2025 21:45:19

115. Ligterink NF, Walsh C, Bhuin RG, Vissapragada S, van Scheltinga JT, Linnartz H. 2018. Methanol ice co-desorption as a mechanism to explain cold methanol in the gas-phase. *Astron. Astrophys.* 612:A88
116. Skouteris D, Balucani N, Ceccarelli C, Faginas Lago N, Codella C, et al. 2019. Interstellar dimethyl ether gas-phase formation: a quantum chemistry and kinetics study. *Mon. Not. R. Astron. Soc.* 482:3567–75
117. Thaddeus P, Gottlieb CA, Gupta H, Brünken S, McCarthy MC, et al. 2008. Laboratory and astronomical detection of the negative molecular ion C_3N^-. *Astrophys. J.* 677:1132–39
118. Anderson JK, Ziurys LM. 2014. Detection of CCN ($X^2\Pi_r$) in IRC+10216: constraining carbon-chain chemistry. *Astrophys. J. Lett.* 795:L1
119. Herbig GH. 1995. The diffuse interstellar bands. *Annu. Rev. Astron. Astrophys.* 33:19–73
120. Berné O, Tielens AG. 2012. Formation of buckminsterfullerene (C_{60}) in interstellar space. *PNAS* 109:401–6
121. Duley WW, Hu A. 2012. Fullerenes and proto-fullerenes in interstellar carbon dust. *Astrophys. J. Lett.* 745:L11
122. Omont A, Bettinger HF. 2021. Intermediate-size fullerenes as degradation products of interstellar polycyclic aromatic hydrocarbons. *Astron. Astrophys.* 650:A193
123. Kwok S, Zhang Y. 2013. Unidentified infrared emission bands: PAHs or MAONs? *Astrophys. J.* 771:5
124. Bernal JJ, Zega TJ, Ziurys LM. 2022. Destructive processing of silicon carbide grains: experimental insights into the formation of interstellar fullerenes and carbon nanotubes. *J. Phys. Chem. A* 126:5761–67
125. Van Winckel H. 2003. Post-AGB stars. *Annu. Rev. Astron. Astrophys.* 41:391–427
126. Mishra N, Boeckl J, Motta N, Iacopi F. 2016. Graphene growth on silicon carbide: a review. *Phys. Status Solid. A* 213:2277–89
127. Goel A, Howard JB, Vander Sande JB. 2004. Size analysis of single fullerene molecules by electron microscopy. *Carbon* 42:1907–15
128. Bernal JJ, Thakur A, Zega TJ, Muralidharan K, Ziurys LM. 2023. On carbon nanotubes as carriers of diffuse interstellar/circumstellar bands. *Astrophys. J.* Submitted
129. Chen T, Xiao CY, Li A, Zhou CT. 2022. Where have all the interstellar silicon carbides gone? *Mon. Not. R. Astron. Soc.* 509:5231–36
130. Benner SA, Kim HJ, Biondi E. 2019. Prebiotic chemistry that could not have happened. *Life* 9:84
131. Maciá E. 2005. The role of phosphorus in chemical evolution. *Chem. Soc. Rev.* 34:691–701
132. Hinkel NR, Hartnett HE, Young PA. 2020. The influence of stellar phosphorus on our understanding of exoplanets and astrobiology. *Astrophys. J. Lett.* 900:L38
133. Pasek MA. 2019. Phosphorus volatility in the early solar nebula. *Icarus* 317:59–65
134. Koelemay LA, Gold KR, Ziurys LM. 2023. Phosphorus-bearing molecules PO and PN at the edge of the Galaxy. *Nature* 623:292–95
135. Ziurys LM. 1987. Detection of interstellar PN: the first phosphorus-bearing species observed in molecular clouds. *Astrophys. J.* 321:L81–85
136. Bernal JJ, Koelemay LA, Ziurys LM. 2021. Detection of PO in Orion-KL: phosphorus chemistry in the plateau outflow. *Astrophys. J.* 906:55
137. Bergner JB, Öberg KI, Walker S, Guzmán VV, Rice TS, et al. 2019. Detection of phosphorus-bearing molecules toward a solar-type protostar. *Astrophys. J. Lett.* 884:L36
138. Rivilla VM, Drozdovskaya MN, Altwegg K, Caselli P, Beltrán MT, et al. 2020. ALMA and ROSINA detections of phosphorus-bearing molecules: the interstellar thread between star-forming regions and comets. *Mon. Not. R. Astron. Soc.* 492:1180–98
139. Guélin M, Cernicharo J, Paubert G, Turner BE. 1990. Free CP in IRC+10216. *Astron. Astrophys.* 230:L9–11
140. Agúndez M, Cernicharo J, Decin L, Encrenaz P, Teyssier D. 2014. Confirmation of circumstellar phosphine. *Astrophys. J. Lett.* 790:L27
141. Koelemay LA, Burton MA, Singh AP, Sheridan PM, Bernal JJ, Ziurys LM. 2022. Laboratory and astronomical detection of the SiP Radical ($X^2\Pi_i$): more circumstellar phosphorus. *Astrophys. J. Lett.* 940:L11
142. Milam SN, Halfen DT, Tenenbaum ED, Apponi AJ, Woolf NJ, Ziurys LM. 2008. Constraining phosphorus chemistry in carbon- and oxygen-rich circumstellar envelopes: observations of PN, HCP, and CP. *Astrophys. J.* 684:618–25

Downloaded from www.annualreviews.org. Guest (guest) IP: 174.18.91.56 On: Fri, 09 May 2025 21:45:19

143. Tenenbaum ED, Woolf NJ, Ziurys LM. 2007. Identification of phosphorus monoxide ($X^2\Pi_r$) in VY Canis Majoris: detection of the first P-O bond in space. *Astrophys. J.* 666:L29–32
144. Ziurys LM, Schmidt DR, Bernal JJ. 2018. New circumstellar sources of PO and PN: the increasing role of phosphorus chemistry in oxygen-rich stars. *Astrophys. J.* 856:169
145. Christiansen JL. 2022. Five thousand exoplanets at the NASA Exoplanet Archive. *Nat. Astron.* 6:516–19
146. Morrison IS, Gowanlock MG. 2015. Extending Galactic Habitable Zone modeling to include the emergence of intelligent life. *Astrobiology* 15:683–96
147. Gonzalez G, Brownlee D, Ward P. 2001. The Galactic Habitable Zone: galactic chemical evolution. *Icarus* 152:185–200
148. Gowanlock MG, Patton DR, McConnell SM. 2011. A model of habitability within the Milky Way Galaxy. *Astrobiology* 11:855–73
149. Bernal JJ, Sephus CD, Ziurys LM. 2021. Methanol at the edge of the Galaxy: new observations to constrain the Galactic Habitable Zone. *Astrophys. J.* 922:106
150. Fontani F, Colzi L, Bizzocchi L, Rivilla VM, Elia D, et al. 2022. CHEMOUT: CHEMical complexity in star-forming regions of the OUTer Galaxy. I. Organic molecules and tracers of star-formation activity. *Astron. Astrophys.* 660:A76

Downloaded from www.annualreviews.org. Guest (guest) IP: 174.18.91.56 On: Fri, 09 May 2025 21:45:19

Downloaded from www.annualreviews.org. Guest (guest) IP: 174.18.91.56 On: Fri, 09 May 2025 21:45:19